Deposition Simulator for Tobacco Aerosol in the Human Respiratory System

Akina MORI, Shigeaki ITO, and Takashi SEKINE

Scientific Product Assessment Center, Japan Tobacco Inc., 6-2, Umegaoka, Aoba-Ku, Yokohama, Japan

INTRODUCTION

The assessment of the health impact of tobacco aerosol requires an understanding of aerosol behavior in the human respiratory tract. Much effort has been made to measure the dosimetry of the constituents of tobacco products. These methods only measure organ-specific or lung lobe-specific dosimetry. An alternative to taking measurements is computational calculation to predict aerosol behavior. There are computational fluid dynamics (CFD) models that predict tobacco aerosol. Their calculation load is so heavy that CFD model is often for site-specific modeling. The multiple-path particle dosimetry (MPPD) model is another option. The MPPD model uses a multiple-path deterministic mathematical approach for each airway and can reduce computational effort. However, there is room to reflect tobacco-consuming behavior that is, 1) withdrawal of a puff from a tobacco product, 2) holding the puff in the mouth, 3) withdrawal of the dilution air, 4) aerosol transport to the deep lung, 5) pause in the lung, and 6) exhalation of the aerosol.

MATERIALS AND METHOD

2. Model developmental method

A revised model was developed based on existing MPPD models (Asgharian et al. 2014, Asgharian et al. 2018a, Asgharian et al. 2018b) by introducing new equations that represent the real-world behavior of tobacco aerosol.

2.1. Mixture of inhaled aerosol in the oral cavity

A puff of tobacco product enters the oral cavity when a negative pressure gradient is created in the mouth. Assuming steady-state transport, the mass balance (i.e., convection-diffusion) equation of a vapor constituent during puff withdrawal in each section of the oral cavity of radial dimension r and axial dimension z is given by

Airflow rate; Vapor concentration; Puff withdrawal; Airway cross-sectional area; Vapor diffusion coefficient; Mass exchange between the droplets and vapor

$$\frac{q}{A}\frac{\partial C_v}{\partial z} = D_v\frac{\partial^2 C_v}{\partial z^2} + D_v\frac{1}{r}\frac{\partial}{\partial r}\left(r\frac{\partial C_v}{\partial r}\right) - \left.\frac{dFC_d m_d}{dt}\right|_{pw} \quad (1)$$

Similarly, the droplet concentration in the oral cavity is found from the mass balance of. Thus,

Droplet concentration; Airway velocity in the direction of gravity; Droplet diffusion coefficient; Coagulation kernel

$$\frac{\partial C_d}{\partial z} = \frac{D_d A}{q}\frac{\partial^2 C_d}{\partial y^2} - \frac{u_g A}{q}\frac{\partial C_d}{\partial y} - \frac{\beta A}{q}C_d^2 \quad (2)$$

During mouth hold, the puff mixture continues to evolve as a result of phase change, droplet coagulation, vapor uptake, and the gravitational settling of the droplets. The transport models for the vapor and droplet are:

$$\frac{\partial C_v}{\partial t} + \left.\frac{dFC_d m_d}{dt}\right|_{mh} = \frac{D_v}{r}\frac{\partial}{\partial r}\left(r\frac{\partial C_v}{\partial r}\right) \quad (3) \qquad \frac{\partial C_d}{\partial t} = D_d\frac{\partial^2 C_d}{\partial y^2} - u_g\frac{\partial C_d}{\partial y} - \beta C_d^2 \quad (4)$$

Mouth hold

2.2. Mixing of the puff in the oral cavity and deep lung

When the puff travels to the deep lung, two types of mixing occur: mixing of the dilution air with the puff at the end of the puff withdrawal and mixing of the inhaled puff with the reserve air in the deep lung.
Inhaled dilution air enters the oral cavity, mixes with the puff, and carries it into the lung. We adopt stirred-tank model of the oral cavity (Fig. 1) to predict the inlet tracheal concentration during inhalation.

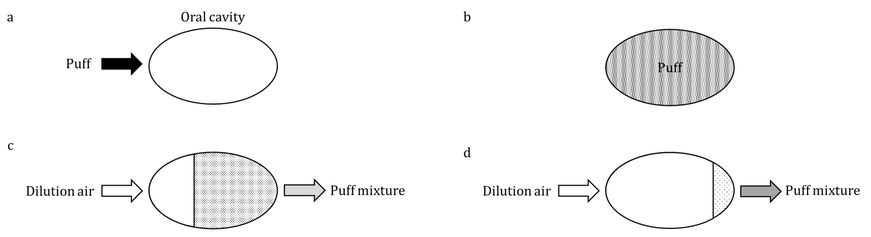

Fig. 1. Stirred-tank model of the oral cavity. (a) puff inhalation into the oral cavity, (b) mouth hold, and (c) and (d) dilution air is inhaled, mixed with the puff in the oral cavity, and leaves at a different concentration.

2.3. Modeling coupled puff transport equations in the lumen and lung tissue

The convective mixing of vapors in an airway made of respiratory bronchioles and alveoli can be accounted for in the mass balance equation for vapors in a simplified model in which the airway contains a lumen and unsmooth space, as shown in Fig. 2. In Fig. 2, A is the duct cross-sectional area and A' is the total cross-sectional area that includes the space in a single respiratory bronchiole. The full set of transport equations during inhalation and exhalation are solved to determine the concentration of vapor in the air and lung tissue.

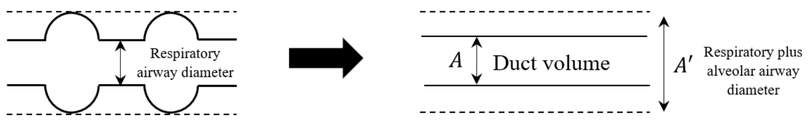

Fig. 2. Idealistic representation of the alveolar region surface.

3. Aerosol conditions input into the model

The constituents and their proportions in a conventional cigarette (CC) aerosol were obtained from the results of chemical analysis (Takahashi et al., 2018) (Table 2). The physicochemical properties of constituents at 37 °C were calculated using a thermodynamic calculator, ProPhyPlus (ProSim, Toulouse, France), and EPA On-line Tools for Site Assessment Calculation (https://www3.epa.gov/ceampubl/learn2model/part-two/onsite/estdiffusion-ext.html).

Table 1. EC aerosol constituents

	Initial mass fraction	Vapor pressure (Pa)	Molecular weight (g/mol)	Density (g/cm3)	Surface tension (dyn/cm)	Diffusion coefficient	Activity coefficient
Water	0.01	6.3×10^{3}	18.0	0.99	70.3	0.28	1.00
Nicotine	0.03	13.4	162.2	1.01	38.6	0.07	1.17
Propylene glycol	0.48	49	76.1	1.02	34.3	0.10	1.05
Glycerol	0.48	8.9×10^{-2}	92.1	1.25	62.2	0.10	1.10

Table 2. CC aerosol constituents

	Initial mass fraction	Vapor pressure (Pa)	Molecular weight (g/mol)	Density (g/cm3)	Surface tension (dyn/cm)	Diffusion coefficient	Activity coefficient
Water	0.734	6.3×10^{3}	18.0	0.99	70.3	0.28	1.12
Nicotine	0.091	13.4	162.2	1.01	38.6	0.07	1.83
Propylene glycol	0.001	49	76.1	1.02	34.3	0.10	3.90
Glycerol	0.113	8.9×10^{-2}	92.1	1.25	62.2	0.10	6.41
Triacetin	0.050	1.1	218.2	1.14	34.9	0.06	8.69
Hydroquinone	0.004	0.2	110.1	1.30	55.6	0.08	0.06
Catechol	0.004	9.7	110.1	1.22	44.3	0.12	0.06
Phenol	0.001	1.4×10^{2}	94.1	1.06	39.5	0.09	0.56
Pyridine	0.001	5.2×10^{3}	79.1	0.97	35.1	0.98	1.42
Styrene	0.001	1.6×10^{3}	104.2	0.89	30.3	0.08	20.32

RESULTS & DISCUSSION

We conducted sensitivity analysis with the input condition assuming an EC.
Fig. 3 shows the growth of droplets while they traveled through the oral passages at different puff withdrawal times. Droplet growth occurred, and the deposition and uptake fractions increased according to the withdrawal time. The longer the puff withdrawal, the slower the flow rate, and the coagulation is inversely proportional to the flow rate. Because droplet growth potentially decreased deposition in Brownian diffusion, the puff withdrawal time also influenced deposition.
The mouth-hold time changed the droplet size, and the dosimetry (Fig. 4). The growth of droplets during mouth hold was relatively small compared with that during puff withdrawal, which suggests that much of the coagulation and hygroscopic growth already occurred during puff withdrawal. It has been reported that the longer the mouth-hold time, the higher the deposition with the CFD model (Feng et al. 2016). Therefore, we suggest that our model appropriately represents the circumstances.
We used the tissue–air partition coefficient (PC_{ta}) for each constituent as an input parameter in the model. As expected, the nicotine deposition and uptake with PC_{ta} = 0.01 was calculated to be lower than that with PC_{ta} = 1 and PC_{ta} = 100. Thus, the use of PC_{ta} is important for calculating the constituent-specific trend of deposition.

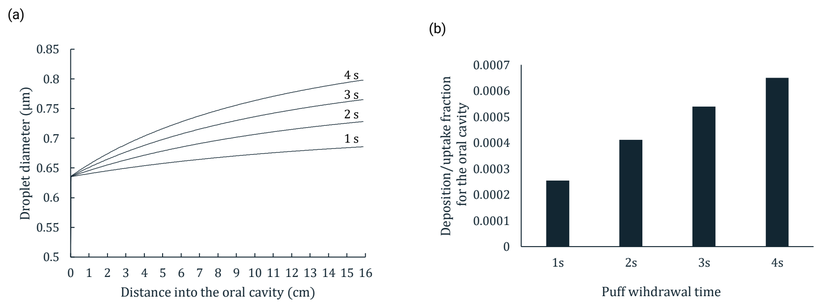

Fig. 3. Effect of the puff withdrawal time:
(a) droplet growth by the time droplets reach the end of the oral cavity and
(b) deposition and uptake fractions of the upper respiratory tract (URT) during puff withdrawal calculated using four puff withdrawal times.

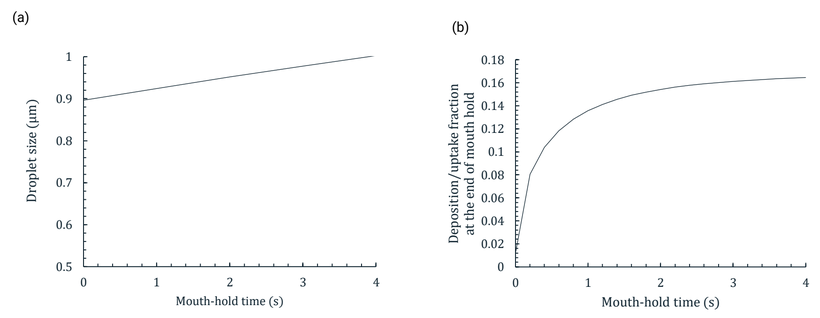

Fig. 4. Effect of the mouth-hold time on (a) droplet growth during mouth hold and (b) the uptake fractions during puff withdrawal and mouth hold.

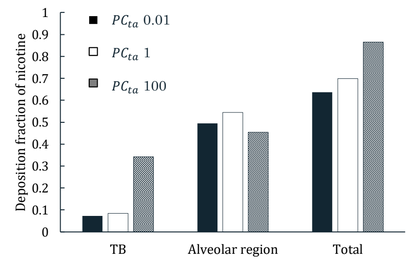

Fig. 5. Influence of the tissue-air partition coefficient for nicotine deposition and uptake.

Fig. 6 and 7 shows the calculation results of dosimetry of EC and CC. In the URT and TB regions, the deposition and uptake fractions changed according to the vapor pressure of each constituent (Table 1). By contrast, in the alveolar region, the deposition and uptake fractions of glycerol and nicotine increased remarkably in deep lung. We suggest that the uptake of vapor is dominant in the URT and TB regions, whereas the deposition of droplets is dominant in deep lung. The deposition and uptake fractions of each constituent of CC in the URT were not completely according to the vapor pressure (Table 2). Because the activity coefficient corrects the vapor pressure, constituents with a high activity coefficient tend to deposit in the URT. Nicotine in the EC was predicted to deposit and be taken up more in the deeper lung, and was maximized in the deepest lung, whereas the 9th airway generation was the vertex in the case of the CC. This was caused by the difference in aerosol properties between the EC and CC in addition to the difference of activity coefficient. The CC had fewer droplets than the EC and the constituents in CC aerosol evaporated more easily than those in EC aerosol, which resulted in the droplet diameter of CC becoming smaller, and nicotine evaporated more than for the EC.
Importantly, we performed these calculations within 3 minutes. A low calculation load is important for a versatile model, and it enables the efficient evaluation of tobacco products with many constituents.

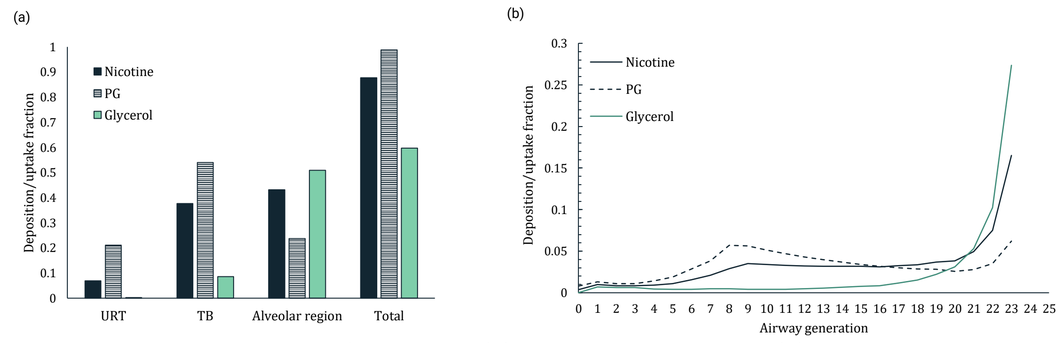

Fig. 6. EC deposition and uptake fractions on (a) each airway region and (b) each airway generation.

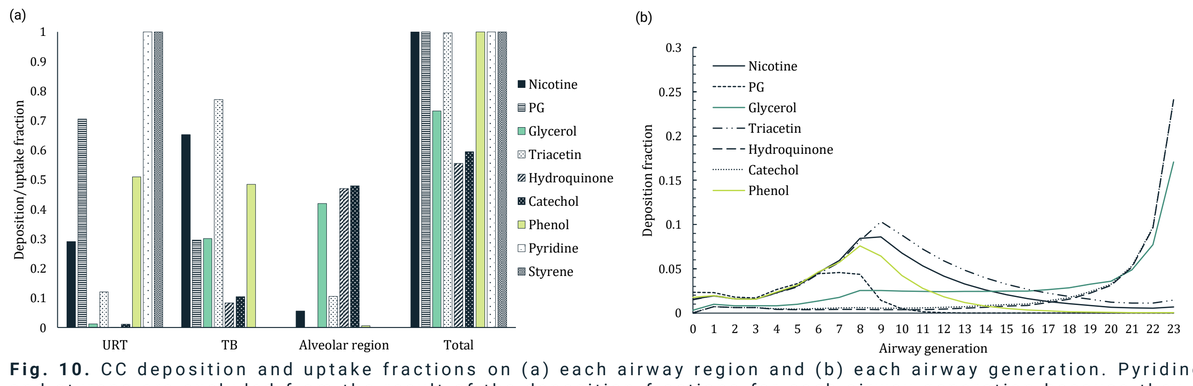

Fig. 10. CC deposition and uptake fractions on (a) each airway region and (b) each airway generation. Pyridine and styrene are excluded from the result of the deposition fractions for each airway generation because they are solely deposited in the URT region.

CONCLUSION

We developed a modified version of MPPD in which we introduced three aerosol dynamics models: dynamics during puff withdrawal and mouth hold, convective mixing in the oral cavity and deep lung, and puff transport between the tissue surface and air. The modified MPPD enables us to calculate the deposition of each chemical constituent of interest in each airway and the generation of the respiratory tract by inputting the physicochemical properties and aerosol properties. We can also reflect the behavior of tobacco product use. Importantly, this model can perform a quick and effective calculation with multiple chemical constituents in aerosol, and the results are generally consistent with the global understanding of aerosol physics and the previous deposition model with CFD. We believe that our model is useful for considering the actual exposure concentration of harmful and potentially harmful constituents in tobacco product aerosol, and expect it to be applied to toxicological studies under the consideration of real-world scenarios, in addition to in vitro to in vivo extrapolation.

REFERENCES

Asgharian, B., Price, O. T., Yurteri, C. U., Dickens, C., & McAughey, J. (2014). Component-specific, cigarette particle deposition modeling in the human respiratory tract. Inhalation Toxicology, 26(1), 36-47. doi: 10.3109/08958378.2013.851305

Asgharian, B., Price, O. T., Rostami, A. A., & Pithawalla, Y. B. (2018b). Deposition of inhaled electronic cigarette aerosol in the human oral cavity. Journal of Aerosol Science, 116, 34-47. doi: 10.1016/j.jaerosci.2017.11.014

Asgharian, B., Rostami, A. A., Price, O. T., & Pithawalla, Y. B. (2018a). Regional deposition of inhaled aerosol constituents from Electronic Nicotine Delivery Systems (ENDS) in the respiratory tract. Journal of Aerosol Science, 126, 7-20. doi: 10.1016/j.jaerosci.2018.08.006

Takahashi, Y., Kanemaru, Y., Fukushima, T., Eguchi, K., Yoshida, S., Miller-Holt, J., & Jones, I. (2018). Chemical analysis and in vitro toxicological evaluation of aerosol from a novel tobacco vapor product: A comparison with cigarette smoke. Regulatory Toxicology and Pharmacology, 92, 94-103. doi: 10.1016/j.yrtph.2017.11.009

Feng, Y., Kleinstreuer, C., Castro, N., & Rostami, A. (2016). Computational transport, phase change and deposition analysis of inhaled multicomponent droplet–vapor mixtures in an idealized human upper lung model. Journal of Aerosol Science, 96, 96-123. doi: 10.1016/j.jaerosci.2016.03.001

Visit www.jt-science.com

JT SCIENCE